The influence of time delay in a chaotic cancer model

Subhas Khajanchi,[1,a)] Matjaž Perc,[2,3,4,b)] and Dibakar Ghosh[5,c)]
[1]*Department of Mathematics, Presidency University, Kolkata 700073, India*
[2]*Faculty of Natural Sciences and Mathematics, University of Maribor, Koroška cesta 160, SI-2000 Maribor, Slovenia*
[3]*School of Electronic and Information Engineering, Beihang University, Beijing 100191, China*
[4]*Complexity Science Hub Vienna, Josefstädterstraße 39, A-1080 Vienna, Austria*
[5]*Physics and Applied Mathematics Unit, Indian Statistical Institute, Kolkata 700108, India*

(Received 18 August 2018; accepted 12 September 2018; published online 1 October 2018)

The tumor-immune interactive dynamics is an evergreen subject that continues to draw attention from applied mathematicians and oncologists, especially so due to the unpredictable growth of tumor cells. In this respect, mathematical modeling promises insights that might help us to better understand this harmful aspect of our biology. With this goal, we here present and study a mathematical model that describes how tumor cells evolve and survive the brief encounter with the immune system, mediated by effector cells and host cells. We focus on the distribution of eigenvalues of the resulting ordinary differential equations, the local stability of the biologically feasible singular points, and the existence of Hopf bifurcations, whereby the time lag is used as the bifurcation parameter. We estimate analytically the length of the time delay to preserve the stability of the period-1 limit cycle, which arises at the Hopf bifurcation point. We also perform numerical simulations, which reveal the rich dynamics of the studied system. We show that the delayed model exhibits periodic oscillations as well as chaotic behavior, which are often indicators of long-term tumor relapse. *Published by AIP Publishing.* https://doi.org/10.1063/1.5052496

Understanding how immune system reacts to the emergence of tumors and their growth is of the outmost importance in oncology and medical research. Typically, the innate and adaptive immune cells suppress the progression of tumor proliferation by either eliminating tumor cells or by attempting to regulate their outgrowth. We here propose and analyze a tumor-immune interaction model that consists of three nonlinear differential equations with a single time-delayed interaction, whereby the time delay describes the time that is necessary for the differentiation and the transportation of cells. We perform detailed analysis of the existence and stability of biologically feasible singular points and the occurrence of Hopf bifurcations in our model. We show that the stability of nonnegative singular points is possible only when the delay is restricted in a particular interval, while Hopf bifurcation towards oscillatory behavior occurs only if the delay is above a critical value. Moreover, our computer simulations demonstrate that in addition to time delay interactions, the model also exhibits deterministic chaos via a typical period-doubling route. Such complex oscillatory solutions may be indicative of long-term tumor relapse, and they also indicate clearly that the incorporation of realistic time delays in cancer models significantly increase the dynamical complexity of the tumor-immune competitive system.

I. INTRODUCTION

Cancer is one of the greatest threats to public health in the world today. Many forms of cancer have reached epidemic scales, and the unchecked proliferation as well as failures to control increasing numbers of those that affect are highly worrying. Cancer is caused by the abnormal growth of normal tissue that invades surrounding parts of our body.[1] The proliferation of tumor cells is a complex process, which depends on different types of mutant (tumor) cells, immune-effector cells (activated cytotoxic-T-lymphocytes, Macrophages, natural-killer cells), host cells, and endothelial cells, to name just a few. In order to understand such complex biological phenomena in terms of crucial parameters which control the system dynamics, theoretical model analysis is required (Gatenby and Maini[2]). Mathematical models give realistic and quantitative characterizations of complicated biological scenarios, and the results provide the understanding of the state of tumor under various conditions.[3] This complexity has attracted the attention of many mathematicians as well as oncologists.[3–6] The concept of using mathematical modeling for tumor dynamics was first established in 1955 by Thomlinson and Gray.[7]

The tumor and anti-tumor dynamical responses in vivo are complicated,[8–13] and the quantifications of these states are almost impossible in vivo dynamics. The proliferation of tumor cells is not always very fast and at a primary stage the tumor could stay of a detectable size (1–3 mm in diameter). Below the threshold level by routine imaging for a long period of time, this phenomenon is designated by "tumor dormancy."[14] The diversity levels of the cancer system (gene, molecular, gene, cellular, etc.), self organization of the system, tumor-microenvironment, and tumor-immune interaction[15,16] make difficult to treat. Theoretically, such complexity induces various types of attractors (singular point, periodic behavior, strange attractor, etc.).[6,11,17] The existence of limit cycle and strange attractor result in a complex dynamics of the tumor-immune system.[18,19] Such strange behavior of tumor

a)Electronic mail: subhas.maths@presiuniv.ac.in
b)Electronic mail: matjaz.perc@gmail.com
c)Electronic mail: diba.ghosh@gmail.com

cells could be described based on the fundamental mechanisms of chaos,[12,20] which is sensitive dependence on the initial values. Sensitive dependence of initial values builds the proliferation of cancer patterns case specific, that is, evolution of tumor varies from patient to patient due to different initial values. This is fairly a challenging problem for the clinicians and oncologists and a very fascinating theme in the field of tumor dynamics. Due to these grounds, chaotic scenario in tumor dynamics could provide an advanced knowledge of this complex interactive process.[11,12]

The patient's immune state with cancer cells often shows rather asymmetrical and is unpredictable due to the complex interaction with cancer cells. How the immune state responses to the establishment and proliferation of tumors is a fascinating and indispensable question in tumor dynamics and immunology. It is well-known to the researchers that the adaptive and cellular immune systems not only suppress the proliferation of tumor but also stimulate the progression and development of tumor.[21–25] The theoretical investigation of tumor and immune interactive dynamics has a long history and a good precis can be observed in Adam and Bellomo.[3]

The delayed responses[26,27] cannot be neglected for the cancer and immune system interplay, just as Villasana and Radunskaya,[19] Moghtadaei *et al.*,[28] Khajanchi,[29] and Bi *et al.*[10] revealed that discrete time lags should be considered to narrate the times required for the development of molecules, progression, differentiation of cell populations, transport, etc. In fact, dynamic relationships between cancer-immune system interplay with time lag have been investigated extensively; see Refs. 10, 11, 19, and 28–35, and the references cited therein.

Villasana and Radunskaya[19] developed a mathematical model to study the tumor-immune competitive system and introduce time lag to investigate the phases for cell-cycle process. Bi *et al.*[10] considered a mathematical model of cancer-immune interplays with three distinct time lags, namely, the growth of cancer cells, proliferation of immune cells activated by cancerous cells, and the differentiation of immune cell population. The authors investigated that three distinct time lags are asymptotically stable if the time lags are less than their critical values and Hopf bifurcation occurs if any one of these time lags crosses its critical value. Khajanchi and Banerjee[11] proposed a delayed cancer model to study the growth of immune cells by cancer cells. In their article, the authors investigated the two-dimensional bifurcation region to clearly understand the intricate behavior of cancer-immune system interplays. Forys and Piotrowska[32] studied a system of angiogenesis models with time delays to describe the angiogenesis process. They introduced external treatment in their tumor model and proved that the external treatment not only decreases the cancer size but also increases the region of stability. Moghtadaei *et al.*[28] investigated the well-known Kuznetsov *et al.*[6] tumor model in a discretized version by introducing Mickens rules for the nonstandard finite difference scheme. The authors investigated the chaotic dynamics, regular and irregular periodic behaviors that exhibit the phenomena for long run tumor relapse.

In the present article, we investigate a mathematical model introduced by Pillis and Radunskaya,[36] which investigate the interactive dynamics between three cells, namely, immune cells, host cells, and tumor cells. The set of parameters were taken to match with biological evidences.[12,36] Therefore, the model could be appraised as qualitatively authenticated with experimental data. The main reason for choosing this model is due to its chaotic behavior[37] which has various similarities to clinical evidences.[12,13,38] In our study, we added a discrete time lag to interplay between cancer and immune effector cells to obtain a better compatibility with real life as the interaction among the cells is not an instantaneous procedure. So it is realistic to introduce a delay in the interaction among tumor and immune effector cells and investigate how the resulting dynamics effects by the delay time. There are medical confirmations that anti-tumor or activity by immunotherapeutic drug is investigated not instant but from 2 to 10 weeks after the initiation of treatments.[39]

The rest of this article is organized as follows: Sec. II is devoted to a short description of the delayed model and its normalization. Section III deals with the qualitative study of the model including solution's positivity and boundedness, local stability analysis of the biologically feasible singular points, occurrence of Hopf bifurcation and estimate the length of time lag to preserve the stability of periodic limit cycle. We numerically studied how this tumor-immune interactive dynamics is influenced by time delay in Sec. IV. One and two parameter bifurcation analysis are investigated in the same section. Section V provides a brief discussion about the main findings of our model.

II. THE MATHEMATICAL MODEL

Over the last three decades, mathematical models have been developed in different aspects of cancer dynamics[5,15,40,41] with different types of interactions. Effector-immune cells are the important elements in the immune system that destroy the tumor cells through a kinetic process by which the tumor cells come in contact with effector cells and making them functionally inactive. Also, the tumor cells secrete immunosuppressive cytokine TGF-β, prostaglandin E2, IL-10, etc. which are able to stimulate the proliferation of tumor cells. Thus, instantaneously, the effector cells are unable to destroy the tumor cells so there is a time lag between the deactivation of tumor cells by immune effector cells. This time lag can be regarded as an interaction delay. To keep this in mind, the model of de Pillis and Radunskaya[36] is thus modified in the delayed system as

$$\begin{cases} \dfrac{dE(T_1)}{dT_1} = \dfrac{\overline{\rho}T(T_1)E(T_1)}{\overline{g}+T(T_1)} - \overline{\beta_1}T(T_1-\tau) \\ \qquad\qquad \times E(T_1-\tau) - \overline{\delta}E(T_1), \\ \dfrac{dH(T_1)}{dT_1} = \overline{\alpha}H(T_1)\left(1-\dfrac{H(T_1)}{k_1}\right) - \overline{\gamma_1}T(T_1)H(T_1), \\ \dfrac{dT(T_1)}{dT_1} = \overline{a}T(T_1)\left(1-\dfrac{T(T_1)}{k_2}\right) - \overline{\beta_2}T(T_1-\tau) \\ \qquad\qquad \times E(T_1-\tau) - \overline{\gamma_2}T(T_1)H(T_1), \end{cases} \quad (1)$$

where $E(T_1)$, $H(T_1)$, and $T(T_1)$ represent the number of immune effector cells, healthy tissue cells or host cells, and tumor cells at time T_1, respectively. The first term in the

first equation of (1) designates the growth of cancer-specific immune cells and is modeled via Michaelis-Menten saturation dynamics to take into account for the self-limiting production of effector immune cells, with $\overline{\rho}$ being the proliferation rate and $\overline{g}$ represents the steepness coefficient. The second term $\overline{\beta_1}T(T_1-\tau)E(T_1-\tau)$ describes the clearance of effector immune cells by tumor cells at the rate $\overline{\beta_1}$. Also, at the same time, the clearance of cancer cells by immune cells occur at the rate $\overline{\beta_2}$ in the third equation. Here, τ is the discrete time lag factor that has been added due to interaction delay. The last term designates the natural decay of immune cells at the rate $\overline{\delta}$. Second equation represents the dynamics of healthy cells or host cells, the first term represents the host cells that can proliferate logistically with the growth rate $\overline{\alpha}$ and k_1 is the carrying capacity. Second term designates the decay of host cells due to interplay with cancer cells with a rate $\overline{\gamma_1}$. The third equation designates the rate of change of tumor cells in which the tumor cells can grow logistically without any immune intervention, with $\overline{a}$ being the proliferation rate and k_2 being an environmental carrying capacity. The final term represents the elimination of cancer cells due to interplay with healthy tissue cells at a rate $\overline{\gamma_2}$.

For the simplicity of (1), we normalize the state variables using the following scaling:

$$[x(t),y(t),z(t)]=\left(\frac{E}{\overline{g}},\frac{H}{k_1},\frac{T}{k_2}\right),\quad \text{with}\quad t=\overline{a}T_1,$$

and we obtain the new parameter set as

$$\rho=\frac{\overline{\rho}}{\overline{a}},\quad g=\frac{\overline{g}}{k_2},\quad \beta_1=\frac{\overline{\beta_1}k_2}{\overline{a}},\quad \delta=\frac{\overline{\delta}}{\overline{a}},$$
$$\alpha=\frac{\overline{\alpha}}{\overline{a}},\quad \gamma_1=\frac{\overline{\gamma_1}k_2}{\overline{a}},\quad \beta_2=\frac{\overline{\beta_2}\overline{g}}{\overline{a}},\quad \gamma_2=\frac{\overline{\gamma_2}k_1}{\overline{a}}.$$

Now, system (1) leads to $(E,H,T)\mapsto(x,y,z)$, where $x(t)$ designates normalized immune cells, $y(t)$ and $z(t)$ are the population of host and cancer cells, respectively, as

$$\begin{cases}\dfrac{dx}{dt}=\dfrac{\rho xz}{g+z}-\beta_1x(t-\tau)z(t-\tau)-\delta x,\\ \dfrac{dy}{dt}=\alpha y(1-y)-\gamma_1yz,\\ \dfrac{dz}{dt}=z(1-z)-\beta_2x(t-\tau)z(t-\tau)-\gamma_2yz,\end{cases}\tag{2}$$

with initial history functions as

$$x(\theta)=\varphi_1(\theta),\quad y(\theta)=\varphi_2(\theta),\quad z(\theta)=\varphi_3(\theta),\tag{3}$$

with $\varphi_i(\theta)\geq 0$, $i=1,2,3$ for $\theta\in[-\tau,0]$, where $\varphi_i(\theta)\in\mathbb{R}^3_+$ are the continuous functions on $[-\tau,0)$ that may display jumps at $\theta=0$.

III. BASIC PROPERTIES OF THE MODEL

In the following lemma, we shall investigate the positive invariance of the delay differential system (2).

Lemma 3.1. *For the nonnegative initial conditions* $(\varphi_i, i=1,2,3)$, *defined on* $[0,+\infty)$, *there exists nonnegative solution of system (2). Moreover, the solution of system (2) is bounded for all* $t\geq 0$.

Proof 3.1. *System (2) can be stated into the vector form as*

$$\dot{X}(t)=\mathcal{M}(X)\quad\text{with}\quad X=[x(t),y(t),z(t)]^T\in\mathbb{R}^3_{+,0}$$

and

$$\mathcal{M}(X)=\begin{pmatrix}\dfrac{\rho xz}{g+z}-\beta_1x(t-\tau)z(t-\tau)-\delta x\\ \alpha y(1-y)-\gamma_1yz\\ z(1-z)-\beta_2x(t-\tau)z(t-\tau)-\gamma_2yz\end{pmatrix}=\begin{pmatrix}\mathcal{M}_1(X)\\ \mathcal{M}_2(X)\\ \mathcal{M}_3(X)\end{pmatrix},$$

where the function $\mathcal{M}:\mathbb{R}^3_+\mapsto\mathbb{R}^3$ *for* $\mathcal{M}\in C^\infty(\mathbb{R}^3_+)$ *defined in the nonnegative octant* $\mathbb{R}^3_+$. *The right side of the above system is locally Lipschitz and satisfy the conditions*

$$\mathcal{M}_i(X)\,|_{X_i(t)}, X\in\mathbb{R}^3_+=\mathcal{M}_i(0)\geq 0\quad\text{for } i=1,2,3.$$

According to the lemma by Yang et al., every solution of system (2) with initial values (3), $\varphi_i(t)\in\mathbb{R}^3_+$, *say,* $X(t)=X[t;X(0)]$, *for all* $t>0$, *that is, it remains positive throughout the region* $\mathbb{R}^3_+$, $\forall\, t>0$.

From the positivity of solutions yields the right side of (2) is given by

$$\frac{dx}{dt}\leq\frac{\rho xz}{g+z}-\delta x.$$

Hence, $x(t)\leq\max\{0,\varphi_1(0)\}$ *if* $\frac{\rho}{\delta}<1$. *Second equation of (2), the positive of solutions yields the right side is bounded due to the proliferation term* $\alpha y(t)[1-y(t)]$. *Hence,*

$$y(t)\leq\max[\varphi_2(0),1].$$

The last equation of (2) leads to

$$z(t)\leq\max[\varphi_3(0),1].$$

Therefore, the solutions of (2) are nonnegative and bounded for all finite times.

A. Equilibria

The tumor model (2) has six biologically meaningful singular points:

1. the no "living cell" singular point $E_0(0,0,0)$.
2. The tumor-free fixed point $E_1(0,\hat{y},0)$ with $\hat{y}=1$.
3. The fixed point $E_2(0,0,\tilde{z})$ with $\tilde{z}=1$, in which only tumor cells are present.
4. The fixed point

$$E_3(\breve{x},0,\breve{z})=\begin{cases}\breve{x}=\dfrac{1-\breve{z}}{\beta_2},\\ \breve{y}=0,\\ \breve{z},\end{cases}$$

in which tumor cells and immune effector cells exist together. The third coordinate $\breve{z}$ is the non-negative

root(s) of

$$\beta_1 \breve{z}^2 + \breve{z}(\delta + g\beta_1 - \rho) + g\delta = 0, \tag{4}$$

which can be written as

$$\breve{z} = \frac{(\rho - \delta - g\beta_1) + \sqrt{(\rho - \delta - g\beta_1)^2 - 4g\delta\beta_1}}{2\beta_1}.$$

The singular point E_3 is feasible if

$$\begin{cases} \rho > \delta + g\beta_1, \\ \breve{z} < 1, \end{cases}$$

that is, effector cells resist against tumor attacks and the death rate of effector cells. In the case of $\breve{z} = 1$, the boundary equilibrium E_3 reduces to E_2 which means the tumor cells always persist in the patients' body.

5. The singular point

$$E_4(0, \bar{y}, \bar{z}) = \begin{cases} \bar{x} = 0, \\ \bar{y} = \dfrac{\gamma_1 - \alpha}{\gamma_1\gamma_2 - \alpha}, \\ \bar{z} = \dfrac{\alpha(\gamma_2 - 1)}{\gamma_1\gamma_2 - \alpha} \end{cases}$$

corresponds to a situation in which cancer cells and host cells coexist. The effector cell free singular point is biologically meaningful if $\gamma_2 > 1$, $\gamma_1 > \alpha$, and $\gamma_1\gamma_2 > \alpha$, which implies that (i) the decay rate of tumor population by host population is greater than unity and (ii) the suppression rate of host population by cancer population is more efficient than the proliferation rate of host cells. For $\gamma_2 = 1$, the singular point E_4 coincide with tumor free equilibrium point E_1.

6. The interior fixed point

$$E^*(x^*, y^*, z^*) = \begin{cases} x^* = \dfrac{\alpha(1 - \gamma_2) + z^*(\gamma_1\gamma_2 - \alpha)}{\alpha\beta_2}, \\ y^* = \dfrac{\alpha - \gamma_1 z^*}{\alpha}, \\ z^*, \end{cases}$$

where z^* is the nonnegative solution of the quadratic Eq. (4). At this singular point, the three cells, namely, cancer, effector, and host cells exist together. The interior fixed point E^* is positive if the conditions hold: $\rho > \delta + g\beta_1$, $\gamma_2 < 1$, $\gamma_1\gamma_2 > \alpha$, and $z^* < \frac{\alpha}{\gamma_1}$. Using the existence conditions of E^*, it is obvious that the immune cell free singular point E_4 will never persist as for the inactivation rate γ_2 of tumor cells violates the existence of effector free singular point E_4.

B. Local asymptotic stability of the singular point

In this subsection, we study the local asymptotic stability of the biologically feasible fixed points of (2) around each of the equilibrium points. In order to do this, we calculate the following Jacobian matrix corresponding to each of the singular points is given by

$$J_E = \begin{pmatrix} j_{11} & 0 & j_{13} \\ 0 & j_{22} & j_{23} \\ j_{31} & j_{32} & j_{33} \end{pmatrix}.$$

where $j_{11} = \frac{\rho z}{g+z} - \delta - \beta_1 z e^{-\lambda\tau}, j_{13} = \frac{g\rho x}{(g+z)^2} - \beta_1 x e^{-\lambda\tau}$, $j_{22} = \alpha(1 - 2y) - \gamma_1 z$, $j_{23} = -\gamma_1 y$, $j_{31} = -\beta_2 z e^{-\lambda\tau}$, $j_{32} = -\gamma_2 z$, and $j_{33} = 1 - 2z - \gamma_2 y - \beta_2 x e^{-\lambda\tau}$.

The eigenvalues corresponding to the fixed point E_0 are $\lambda_1^0 = -\delta(< 0)$, $\lambda_2^0 = -\alpha(< 0)$, and $\lambda_3^0 = 1(> 0)$. Therefore, E_0 is a saddle point in the 2-dimensional stable manifold and 1-dimensional unstable manifold. Thus, there is no path emanating in the nonnegative octant which can converge to E_0.

The eigenvalues corresponding to E_1 are $\lambda_1^1 = -\delta(< 0)$, $\lambda_2^1 = -\alpha(< 0)$, and $\lambda_3^1 = 1 - \gamma_2$. The tumor-free singular point E_1 is locally asymptotically stable if $\lambda_3^1 < 0$, that is, if $\gamma_2 > 1$. Otherwise, the system will be unstable. It can be observed that if E_1 is stable, the singular point E_4 and the interior fixed point E^* do not exist. Furthermore, for the set of parameters, the cancer-free state leads to a point attractor, there no longer persists a possibility of a sustained cancer proliferation, the micro-environment is not conducive to the proliferation of cancer cells.

At $E_2(0, 0, 1)$, the eigenvalues are $\lambda_1^2 = \frac{\rho}{g+1} - \beta_1 - \delta$, $\lambda_2^2 = \alpha - \gamma_1$, and $\lambda_3^2 = -1$. Therefore, E_2 is locally asymptotically stable for $\rho < (\beta_1 + \delta)(g + 1)$ with $\gamma_1 > \alpha$. These conditions describe that the effector and healthy cells are not growing properly in surviving for colonize tumor, cancer cells remain as single cells in the site. Otherwise, when proliferation rate of immune effector cells and the healthy cells are sufficiently strong to control the growth of cancer cells, this equilibrium point E_2 is unstable in nature, which is thus an non-viable state to reach. The cancer cells cannot proliferate rapidly since the cancer cells remain in competition with the micro-environment.

At $E_3(\breve{x}, 0, \breve{z})$, the characteristic values of J_{E_3} are $\lambda_1^3 = \alpha - \gamma_1\breve{z}$ and the other two eigenvalues $\lambda_{2,3}^3$ are the roots of the following characteristics equation $\lambda^2 + D_1\lambda + D_2 = 0$, where

$$\begin{cases} D_1 = \delta + \beta_1\breve{z} + \beta_2\breve{x} + 2\breve{z} - 1 - \dfrac{\rho\breve{z}}{g + \breve{z}}; \\ D_2 = \left(\dfrac{\rho\breve{z}}{g + \breve{z}} - \beta_1\breve{z} - \delta\right)(1 - \beta_2\breve{x} - 2\breve{z}) \\ \qquad + \beta_2\breve{z}\left(\dfrac{g\rho\breve{x}}{(g + \breve{z})^2} - \beta_1\breve{x}\right). \end{cases}$$

The boundary equilibrium point E_3 will be asymptotically stable if $D_1 > 0, D_2 > 0$, and $\breve{z} > \frac{\alpha}{\gamma_1}$, otherwise unstable.

At $E_4(0, \bar{y}, \bar{z})$, the characteristic values of J_{E_4} are $\lambda_1^4 = \frac{\rho\bar{z}}{g+\bar{z}} - \beta_1\bar{z} - \delta$ and other two eigenvalues $\lambda_{2,3}^4$ are the roots of the following characteristics equation $\lambda^2 + C_1\lambda + C_2 = 0$, where

$$\begin{cases} C_1 = 2\bar{z} + \gamma_2\bar{y} + \alpha\bar{y} - 1; \\ C_2 = \alpha\bar{y}(2\bar{z} + \gamma_2\bar{y} - 1) - \gamma_1\gamma_2\bar{y}\bar{z}. \end{cases}$$

The equilibrium point E_4 will be asymptotically stable if $C_1 > 0, C_2 > 0$, and $\lambda_1^4 < 0$. Thus, the effector cell free

singular point $E_4(0, \bar{y}, \bar{z})$ is stable asymptotically for

$$\begin{cases} \rho\alpha(\gamma_2-1)(\gamma_1\gamma_2-\alpha) < \alpha(\beta_1 g+\delta)(\gamma_2-1)(\gamma_1\gamma_2-\alpha) \\ \quad +\alpha^2\beta_1(\gamma_2-1)^1+\delta g(\gamma_1\gamma_2-\alpha)^2, \\ \dfrac{\alpha+\gamma_2}{1+\gamma_1} > 1, \\ \gamma_2(\alpha+\gamma_1) > (\alpha+\gamma_1\gamma_2^2). \end{cases}$$

Now, our aim is to explore the influence of discrete time lag when all the three cells coexist, that is, the dynamical behavior of system (2) around the interior fixed point $E^*(x^*, y^*, z^*)$. For the case of discrete time lag τ, the characteristic polynomial of the linearized system around $E^*(x^*, y^*, z^*)$ can be written as

$$A(\lambda) + B(\lambda)e^{-\lambda\tau} = 0, \tag{5}$$

where

$$\begin{cases} A(\lambda) = \lambda^3 + a_1\lambda^2 + a_2\lambda + a_3, \\ B(\lambda) = b_1\lambda^2 + b_2\lambda + b_3, \end{cases}$$

with

$$\begin{cases} a_1 = \delta + (\alpha+\gamma_2)y^* + 2z^* - 1 - \dfrac{\rho z^*}{g+z^*}, \\ a_2 = \alpha y^*(\gamma_2 y^* + 2z^* - 1) - \gamma_1\gamma_2 y^* z^* \\ \qquad + \{(\alpha+\gamma_2)y^* + 2z^* - 1\}\left(\delta - \dfrac{\rho z^*}{g+z^*}\right), \\ a_3 = \left(\delta - \dfrac{\rho z^*}{g+z^*}\right)[\alpha y^*(\gamma_2 y^* + 2z^* - 1) - \gamma_1\gamma_2 y^* z^*], \\ b_1 = \beta_2 x^* + \beta_1 z^*, \\ b_2 = \alpha\beta_2 x^* y^* + (\alpha y^* + \gamma_2 y^* + 2z^* - 1)\beta_1 z^* \\ \qquad + \beta_2 x^*\left(\delta - \dfrac{\rho z^*}{g+z^*}\right) + \beta_2 z^*\dfrac{g\rho x^*}{(g+z^*)^2}, \\ b_3 = \alpha y^*(\gamma_2 y^* + 2z^* - 1)\beta_1 z^* - \gamma_1\gamma_2 y^*(z^*)^2 \\ \qquad + \alpha\beta_2 x^* y^* z^*\dfrac{g\rho}{(g+z^*)^2} + \left(\delta - \dfrac{\rho z^*}{g+z^*}\right)\alpha\beta_2 x^* y^*. \end{cases}$$

Without any loss of generality, in the case of interior singular point E^*, that is, in the absence of time lag ($\tau = 0$), characteristic Eq. (5) becomes

$$\lambda^3 + (a_1+b_1)\lambda^2 + (a_2+b_2)\lambda + (a_3+b_3) = 0. \tag{6}$$

Using Routh-Hurwitz criterion, the roots of (6) have non-positive real parts, that is, E^* is asymptotically stable for $a_1 + b_1 > 0$, $S_1 = a_3 + b_3 > 0$, and $S_2 = (a_1 + b_1)(a_2 + b_2) - (a_3 + b_3) > 0$. Then,

$$\begin{aligned} a_1 + b_1 &= \delta + (\alpha+\gamma_2)y^* + z^*(2+\beta_1) + \beta_2 x^* \\ &\quad - 1 - \frac{\rho z^*}{g+z^*} > 0, \\ a_3 + b_3 &= \alpha y^*(\gamma_2 y^* + 2z^* - 1)\left(\beta_1 z^* + \delta - \frac{\rho z^*}{g+z^*}\right) \\ &\quad + y^*(\alpha\beta_2 x^* - \gamma_1\gamma_2 z^*)\left(\delta - \frac{\rho z^*}{g+z^*}\right) \\ &\quad + y^* z^*\left(\alpha\beta_2 x^*\frac{g\rho}{(g+z^*)^2} - \gamma_1\gamma_2\beta_1 z^*\right) > 0, \\ S_2 &= \left[\delta + (\alpha+\gamma_2)y^* + z^*(2+\beta_1)\right. \\ &\quad \left. + \beta_2 x^* - 1 - \frac{\rho z^*}{g+z^*}\right] \\ &\quad \times \left[(\gamma_2 y^* + 2z^* - 1)\left(\alpha y^* + \beta_1 z^* + \delta - \frac{\rho z^*}{g+z^*}\right)\right. \\ &\quad + (\alpha y^* + \beta_1 x^*)\left(\delta - \frac{\rho z^*}{g+z^*}\right) + y^* z^*(\alpha\beta_1 - \gamma_1\gamma_2) \\ &\quad \left. + \beta_2 x^*\left(\alpha y^* + \frac{g\rho z^*}{(g+z^*)^2}\right)\right] - S_1 > 0. \end{aligned} \tag{7}$$

From these expressions, it is difficult to find the explicit parametric criteria which is essential for asymptotic stability of the interior fixed point E^*. We will display this results with the help of numerical simulations.

In the foregoing sections, we studied the dynamics of system (2) without the delay parameter τ. Now onwards, we shall analyze how the stability is influenced by discrete time lag τ and, hence, we examine τ as the bifurcation parameter. To study the delay induced instability, we assume a purely imaginary root of (5).

Now, we are looking for periodic solutions which has a biological relevance in the tumor and immune interactive dynamics (Jeff's phenomenon).[42] To obtain the periodic solutions of (2), we substitute $\lambda = i\sigma (\sigma > 0)$ into (5) and by extracting the real and imaginary parts, we get the following transcendental equations:

$$\begin{aligned} a_1\sigma^2 - a_3 &= (b_3 - b_1\sigma^2)cos(\sigma\tau) + b_2\sigma sin(\sigma\tau), \\ \sigma^3 - a_2\sigma &= b_2\sigma cos(\sigma\tau) - (b_3 - b_1\sigma^2)sin(\sigma\tau). \end{aligned} \tag{8}$$

By squaring and adding both sides of (8), we get

$$\sigma^6 + u_1\sigma^4 + u_2\sigma^2 + u_3 = 0, \tag{9}$$

where

$$\begin{cases} u_1 = a_1^2 - 2a_2 - b_1^2 \\ \quad = \left[\delta + (\alpha+\gamma_2)y^* + 2z^* - 1 - \dfrac{\rho z^*}{g+z^*}\right]^2 \\ \quad - (\beta_2 x^* + \beta_1 z^*)^2 - 2[\alpha y^*(\gamma_2 y^* + 2z^* - 1) \\ \quad - \gamma_1\gamma_2 y^* z^*] + 2\{(\alpha+\gamma_2)y^* + 2z^* - 1\}\left(\delta - \dfrac{\rho z^*}{g+z^*}\right), \\ u_2 = a_2^2 - 2a_1a_3 + 2b_1b_3 - b_2^2, \quad u_3 = a_3^2 - b_3^2. \end{cases}$$

The simplest assumption that Eq. (9) will have a positive root if $u_1 > 0$ and $u_3 = (a_3^2 - b_3^2) = (a_3 + b_3)(a_3 - b_3) < 0$.

From the above conditions, it is obvious that there is a unique non-negative root σ_0 satisfying Eq. (9), i.e., the characteristic polynomial (5) has a pair of purely complex roots in the form $\pm i\sigma_0$. Solving both the equations of (8), we have

$$tan(\sigma\tau) = \frac{b_2\sigma(a_1\sigma^2 - a_3) - (\sigma^3 - a_2\sigma)(b_3 - b_1\sigma^2)}{(a_1\sigma^2 - a_3)(b_3 - b_1\sigma^2) + b_2\sigma(\sigma^3 - a_2\sigma)}.$$

Then, τ_c corresponding to σ_0 is given by

$$\tau_c = \frac{1}{\sigma_0}\arctan\left[\frac{b_2\sigma_0(a_1\sigma_0^2 - a_3) - (\sigma_0^3 - a_2\sigma_0)(b_3 - b_1\sigma_0^2)}{(a_1\sigma_0^2 - a_3)(b_3 - b_1\sigma_0^2) + b_2\sigma_0(\sigma_0^3 - a_2\sigma_0)}\right] + \frac{2c\pi}{\sigma_0}, \quad c = 0, 1, 2, 3, \ldots. \tag{10}$$

For $\tau_c = 0$, the three-cell equilibrium point E^* is locally asymptotically stable, provided condition (7) holds. Hence, by well-known Butler's lemma,[43] E^* will remain stable for $\tau_c < \tau_0$, where $\tau_c = \tau^*$ at $c = 0$. This implies that with a time lag beyond a given critical value, the interaction between cancer cells and their micro-environment begins to lose their stability and, hence, the growth of cancer cells is no longer sustained, making possible fast proliferation of cancer cells.

C. Analysis of Hopf bifurcation

We now establish the onset of a Hopf bifurcation[11] of (2) at $\tau = \tau_c$ when there is a pair of purely imaginary roots, and for which we want to prove the transversality conditions $\frac{d(Re\lambda)}{d\tau}|_{\tau=\tau_c} > 0$. This implies that there exists at least one characteristic value with a positive real part satisfying $\tau > \tau_c$. At first, we are looking for purely complex roots of the form $\lambda = i\sigma_0$ of (5) implying that $|P(i\sigma_0)| = |Q(i\sigma_0)|$, which determines the possible values for τ_c.[44] Now, our objective is to establish the direction of motion of λ when τ_c is increased, for that we need to investigate

$$\Theta = sign\left[\frac{d(Re\lambda)}{d\tau_c}\right]_{\lambda=i\sigma_0} = sign\left[Re\left(\frac{d\lambda}{d\tau_c}\right)^{-1}\right]_{\lambda=i\sigma_0}.$$

Differentiation of (5) with respect to τ leads to

$$[(3\lambda^2 + 2a_1\lambda + a_2) + e^{-\lambda\tau_c}(2b_1\lambda + b_2) - \tau e^{-\lambda\tau_c}(b_1\lambda^2 + b_2\lambda + b_3)]\frac{d\lambda}{d\tau_c} = \lambda e^{-\lambda\tau_c}(b_1\lambda^2 + b_2\lambda + b_3),$$

which implies

$$\left(\frac{d\lambda}{d\tau_c}\right)^{-1} = \frac{2\lambda^3 + a_1\lambda^2 - a_3}{-\lambda^2(\lambda^3 + a_1\lambda^2 + a_2\lambda + a_3)} + \frac{b_1\lambda^2 - b_3}{\lambda^2(b_1\lambda^2 + b_2\lambda + b_3)} - \frac{\tau_c}{\lambda}.$$

Thus,

$$\begin{aligned}\Theta &= sign\left[Re\left(\frac{2\lambda^3 + a_1\lambda^2 - a_3}{-\lambda^2(\lambda^3 + a_1\lambda^2 + a_2\lambda + a_3)} + \frac{b_1\lambda^2 - b_3}{\lambda^2(b_1\lambda^2 + b_2\lambda + b_3)} - \frac{\tau_c}{\lambda}\right)\right]_{\lambda=i\sigma_0} \\ &= \frac{1}{\sigma_0^2}sign\left[\frac{(a_1\sigma_0^2 + a_3)(a_1\sigma_0^2 - a_3) + 2\sigma_0^3(\sigma_0^3 - a_2\sigma_0) + (b_1\sigma_0^2 + b_3)(b_3 - b_1\sigma_0^2)}{b_2^2\sigma_0^2 + (b_3 - b_1\sigma_0^2)^2}\right] \\ &= \frac{1}{\sigma_0^2}sign\left[\frac{2\sigma_0^6 + \sigma_0^4(a_1^2 - 2a_2 - b_1^2) + (b_3^2 - a_3^2)}{b_2^2\sigma_0^2 + (b_3 - b_1\sigma_0^2)^2}\right].\end{aligned}$$

Therefore, the transversality condition $\frac{d(Re\lambda)}{d\tau}|_{\sigma=\sigma_0,\tau=\tau_c} > 0$ holds as $a_1^2 - 2a_2 - b_1^2 > 0$ and $b_3^2 - a_3^2 > 0$ by virtue of $u_1 > 0$ and $u_3 > 0$. The delay induced cancer and immune system model exhibits periodic behavior with small amplitude and bifurcates from three cells singular point E^* when the time delay τ_c as the bifurcation parameter crosses through the threshold value $\tau = \tau_c$. The above outcomes can be precised in the form of the following proposition.

Proposition 3.1. *The existence of three cell singular point E^* with initial conditions (3) are satisfied system (2). Then,*

(i) *if τ lying between $[0, \tau_c)$, then E^* is asymptotically stable,*
(ii) *if $\tau > \tau_c$, then the three-cells singular point E^* is unstable,*
(iii) *at $\tau = \tau_c$, then system (2) experiences Hopf bifurcation around E^*.*

D. Stability of limit cycle: Length of time lag estimation

In this subsection, we explore the stability of bifurcating periodic solutions and estimate the length of time lag preserving the stability of period-1 limit cycle. Consider the tumor model (2) and the space of all continuous real-valued function defined on $[-\tau, +\infty)$, which satisfies the initial history (3) on the interval $[-\tau, 0)$. First, we linearize the tumor model (2) around the interior fixed point $E^*(x^*, y^*, z^*)$, which gives us

$$\begin{cases} \dot{x} = \dfrac{\rho z^*}{g + z^*}x - \delta x - \beta_1 z^* x(t - \tau) \\ \qquad + \dfrac{g\rho x^*}{(g + z^*)^2}z - \beta_1 x^* z(t - \tau), \\ \dot{y} = -\alpha y^* y - \gamma_1 y^* z, \\ \dot{z} = -\beta_2 z^* x(t - \tau) - \gamma_2 z^* y + (1 - 2z^* - \gamma_2 y^*)z \\ \qquad -\beta_2 x^* z(t - \tau). \end{cases} \tag{11}$$

By using Laplace transformation of (11), leading to

$$\begin{cases} (\eta+\delta-\dfrac{\rho z^*}{g+z^*}+\beta_1 z^* e^{-\eta\tau})L_x(\eta) \\ \quad =\dfrac{g\rho x^*}{(g+z^*)^2}L_z(\eta)-\beta_1 z^* e^{-\eta\tau}K_x(\eta)-\beta_1 x^* e^{-\eta\tau}L_z(\eta) \\ \quad -\beta_1 x^* e^{-\eta\tau}K_z(\eta)+\bar{x}(0), \\ (\eta+\alpha y^*)L_y(\eta)=-\gamma_1 y^* L_z(\eta)+\bar{y}(0), \\ (\eta+1-2z^*-\gamma_2 y^*+\beta_2 x^* e^{-\eta\tau})L_z(\eta) \\ \quad =-\beta_2 z^* e^{-\eta\tau}L_x(\eta)-\beta_2 z^* e^{-\eta\tau}K_x(\eta)-\gamma_2 z^* L_y(\eta) \\ \quad -\beta_2 x^* e^{-\eta\tau}K_z(\eta)+\bar{z}(0), \end{cases} \tag{12}$$

with

$$K_x(\eta)=\int_{-\tau}^{0} e^{-\eta t}x(t)dt, \quad K_z(\eta)=\int_{-\tau}^{0} e^{-\eta t}z(t)dt,$$

where $L_x(\eta), L_y(\eta)$, and $L_z(\eta)$ are the respective Laplace transformations of $x(t), y(t)$, and $z(t)$. According to the well-known theory by Freedman *et al.*[43] and using classical Nyquist criteria, three-cells fixed point E^* is asymptotically stable, for

$$ReB(i\xi_0)=0, \tag{13}$$

$$ImB(i\xi_0)>0, \tag{14}$$

with

$$B(\eta)=\eta^3+a_1\eta^2+a_2\eta+a_3+e^{-\eta\tau}(b_1\eta^2+b_2\eta+b_3)$$

and the minimal nonnegative root of the above expressions (13) and (14) is $\xi_0>0$.

Expressions (13) and (14) can be explicitly written as

$$-a_1\xi_0^2+a_3=-b_2\xi_0 sin(\xi_0\tau)-(b_3-b_1\xi_0^2)cos(\xi_0\tau), \tag{15}$$

$$-\xi_0^3+a_2\xi_0>(b_3-b_1\xi_0^2)sin(\xi_0\tau)-b_2\xi_0 cos(\xi_0\tau), \tag{16}$$

which gives sufficient conditions for the stability of interior fixed point E^*. To calculate time lag τ, we employ both conditions (15) and (16). Now, our aim is to investigate an upper bound ξ_+ on ξ_0 that is not dependent on τ, and so to calculate the length of τ, we assume that (16) satisfies $\forall$ values of ξ, $0\le\xi\le\xi_+$ at $\xi=\xi_0$.

Rewriting expression (15) leads to

$$a_1\xi_0^2=a_3+b_2\xi_0 sin(\xi_0\tau)+b_3 cos(\xi_0\tau)-b_1\xi_0^2 cos(\xi_0\tau). \tag{17}$$

To estimate the value of delay, we maximize the right side of (17) as

$$a_3+b_2\xi_0 sin(\xi_0\tau)+b_3 cos(\xi_0\tau)-b_1\xi_0^2 cos(\xi_0\tau),$$

subject to the conditions,

$$|\,cos(\xi_0\tau)\,|\le 1, \quad |\,sin(\xi_0\tau)\,|\le 1.$$

Therefore, we obtain that

$$|\,a_1\,|\,\xi_0^2\le|\,a_3\,|+|\,b_2\,|\,\xi_0+|\,b_3\,|+|\,b_1\,|\,\xi_0^2.$$

Hence, it can be expressed as

$$\xi_+\le\frac{1}{2(|\,a_1\,|-|\,b_1\,|)}\left[|\,b_2\,|+\sqrt{b_2^2+4(|\,a_1\,|-|\,b_1\,|)(|\,a_3\,|+|\,b_3\,|)}\right], \tag{18}$$

then it is obvious from (18) that $\xi_0\le\xi_+$.

Also, from the inequality (16), we have

$$\xi_0^2<a_2+b_2cos(\xi_0\tau)+b_1\xi_0 sin(\xi_0\tau)-\frac{b_3 sin(\xi_0\tau)}{\xi_0}. \tag{19}$$

For the case of $\tau=0$, the above inequality becomes $\xi_0^2<a_2+b_2$ and from (17); $a_1\xi_0^2=a_3+b_3-b_1\xi_0^2$, that is, $\xi_0^2=(a_3+b_3)/(a_1+b_1)$. Therefore, we can assert that at $\tau=0$, the singular point E^* is asymptotically stable if $(a_3+b_3)<(a_1+b_1)(a_2+b_2)$ holds. Now, for small $\tau>0$, (19) will continue to hold.

Putting (17) into (19) and rearranging the expressions, we get

$$\begin{aligned} &(b_3-b_1\xi_0^2-a_1b_2)[cos(\xi_0\tau)-1] \\ &\quad+\left[(b_2-a_1b_1)\xi_0+\frac{a_1b_3}{\xi_0}\right]sin(\xi_0\tau)<a_1a_2-a_3 \\ &\quad+a_1b_2-b_3+b_1\xi_0^2, \\ &\Rightarrow(b_3-b_1\xi_0^2-a_1b_2)[cos(\xi_0\tau)-1] \\ &\quad+\left[(b_2-a_1b_1)\xi_0+\frac{a_1b_3}{\xi_0}\right]sin(\xi_0\tau) \\ &\quad<(a_1+b_1)(a_2+b_2)-(a_3+b_3). \end{aligned} \tag{20}$$

Using the bounds, we obtain

$$\begin{aligned} &(b_3-b_1\xi_0^2-a_1b_2)[\cos(\xi_0\tau)-1] \\ &\quad=2(b_1\xi_0^2+a_1b_2-b_3)sin^2\left(\frac{\xi_0\tau}{2}\right) \\ &\quad\le\frac{1}{2}\xi_+^2\,|\,(b_1\xi_+^2+a_1b_2-b_3)\,|\,\tau^2 \end{aligned}$$

and

$$\begin{aligned} &\left[(b_2-a_1b_1)\xi_0+\frac{a_1b_3}{\xi_0}\right]\sin(\xi_0\tau) \\ &\quad\le\left[\,|\,(b_2-a_1b_1)\,|\,\xi_+^2+|\,a_1\,||\,b_3\,|\,\right]\tau_M. \end{aligned}$$

From (20), we obtain that $D_1\tau^2+D_2\tau\le D_3$, with

$$\begin{aligned} D_1&=\frac{1}{2}\,|\,(b_1\xi_+^2+a_1b_2-b_3)\,|\,\xi_+^2, \\ D_2&=\left[\,|\,(b_2-a_1b_1)\,|\,\xi_+^2+|\,a_1\,||\,b_3\,|\,\right], \\ D_3&=(a_1+b_1)(a_2+b_2)-(a_3+b_3). \end{aligned}$$

Now, it follows that $\tau_+=\frac{1}{2D_1}\left[-D_2+\sqrt{D_2^2+4D_1D_3}\right]$ also for $0\le\tau\le\tau_+$, the Nyquist criteria holds, and the maximum length of time lag τ_+ preserves the stability of period-1 limit cycle.

TABLE I. Explanation of the system parameters.

Name	Definition of parameters	Values
ρ	Maximum recruitment of effector cells	4.5
g	Steepness coefficient of immune cells	1.0
β_1	Fractional immune cell kill by tumor cells	0.2
δ	Decay rate of immune effector cells	0.5
α	Proliferation rate of host cells	0.5
γ_1	Fractional host cell kill by tumor cells	1.5
β_2	Tumor cells inactivation rate	2.5
γ_2	Deactivation rate of tumor cells	1.0

IV. RESULTS AND BIOLOGICAL INTERPRETATIONS

In this section, we represent some numerical computations of our tumor model and provide plausible explanations based on the theoretical outcomes. Parameters and units are arbitrary and we choose those used in Refs. 12 and 33. To see how discrete time delay affects the dynamics of system (2), we choose the parameter set as reported in Table I. For these set of parameters, there are five biologically relevant equilibrium points:

$$E_0 = \begin{vmatrix} x_0 = 0 \\ y_0 = 0 \\ z_0 = 0, \end{vmatrix} \quad E_1 = \begin{vmatrix} \hat{x} = 0 \\ \hat{y} = 1 \\ \hat{z} = 0, \end{vmatrix} \quad E_2 = \begin{vmatrix} \tilde{x} = 0 \\ \tilde{y} = 0 \\ \tilde{z} = 1, \end{vmatrix}$$

$$E_3 = \begin{vmatrix} \breve{x} = 0.346999 \\ \breve{y} = 0 \\ \breve{z} = 0.132503, \end{vmatrix} \quad E^* = \begin{vmatrix} x^* = 0.106002 \\ y^* = 0.602491 \\ z^* = 0.132503. \end{vmatrix}$$

The stabilities of the these equilibrium points with biological interpretations are as follows:

- the corresponding eigenvalues of E_0 are $-0.5, 0.5, 1.0$, then, the critical point is saddle type.
- The tumor free singular point E_1 has eigenvalues $-0.5, -0.5, 0.0$; this indicates a marginally stable node. For $x = z = 0$, that is, only healthy cells exist, the system dynamics dominated by a logistic growth function and host cells converge to its largest value ($y = 1$) [see phase diagram Fig. 1(c)].
- The tumor cells singular point E_2 has eigenvalues $-1.0, -1.0, 1.55$, thus corresponding to a saddle point. In this case, only cancer cells are controlled by a logistic growth equation and the tumor population converges to its largest value ($z = 1$) [see phase diagram Fig. 1(c)].
- The critical point E_3 is a state where immune effector cells and tumor cells coexist. The eigenvalues of E_3 are $0.301246, -0.0662518 \pm 0.613124$ i, which correspond to a saddle focus.
- The interior equilibrium point E^* has eigenvalues—$0.500742, 0.033497 \pm 0.262241$ i, which correspond to a saddle point. The singular point E_3 is 1-dimensional unstable manifold, in this regard, the fixed point E_3 differs from the fixed point E^* which has a 2-dimensional unstable manifold.

To visualize the stability of the fixed points for system (2), we computed the stability region for the recruitment of immune effector cells ρ against the inactivation rate of host cells γ_1 (see Fig. 2). The blue region represents the stability for the boundary fixed point E_3, magenta shaded region indicates the stability of E_2, red shaded region represents the stability of E^*, whereas the white portion indicates the unstable region.

For the specified parameters in Table I, interior singular point E^* is such that $u_1 = 0.263528 > 0$ and $u_3 = -0.0003919 < 0$, which implies that Eq. (9) has exactly one positive real root $\sigma_0 = 0.197656$ and $\tau_0 \approx 0.23425$. Using Proposition 3.1, we obtained that model (2) experiences a

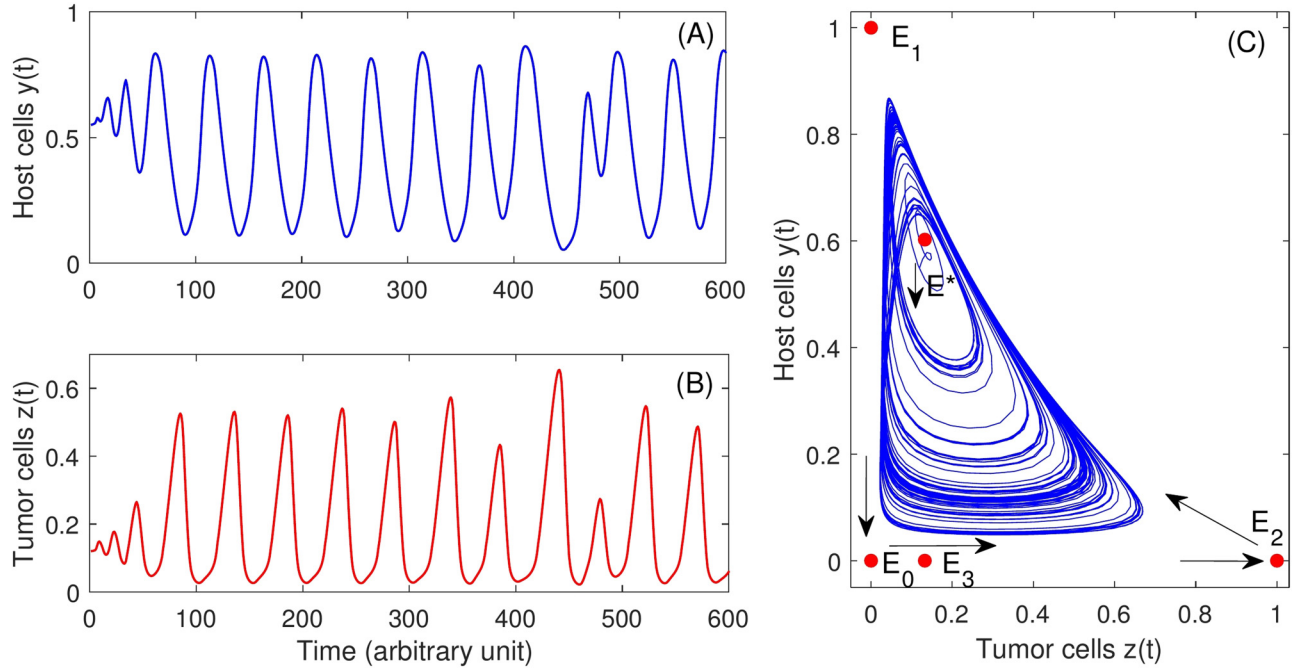

FIG. 1. (a) and (b) depict time evolution of healthy cells and cancer cells for the singular point E^* of the delayed system (2), with time delay $\overline{\tau} = 0.12 (< \tau = 0.2342)$. (c) Represents the 2-dimensional phase portrait diagram for $\overline{\tau} = 0.12 (< \tau = 0.2342)$. Parameter values as reported in Table I.

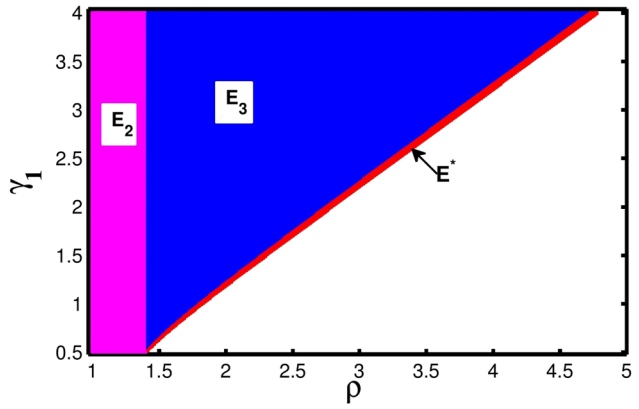

FIG. 2. Stability region for the model (2) for the singular points E_2, E_3, and E^*. The recruitment of immune effector cells ρ versus the host cells inactivation rate γ_1 is plotted. Parameter values as specified in Table I with $\tau = 0$. The blue shaded region represents the stability for E_3, magenta shaded region indicates the stability for E_2, red shaded region represents the stability for E^*, whereas the white portion indicates the unstable region.

Hopf bifurcation at $\tau_0 = 0.23$. We also verified the transversality condition for Hopf bifurcation $\frac{d(Re\lambda)}{d\tau}|_{\sigma=\sigma_0,\tau=\tau_0} = 0.678596 > 0$. According to the well-known Theorem by Cooke and Van den Driessche,[44] it is obvious that system (2) experiences Hopf bifurcation for the increased value of τ, and at $\tau_0 \approx 0.23425$. The stability of (2) changes at $\tau_0 \approx 0.23425$, beyond the threshold value of τ_0, the tumor model reaches to a stable equilibrium state and below the critical value of τ_0 the system exhibits irregular periodic oscillations (chaotic behavior). We also compute the length of time lag τ to preserve the stability of bifurcating limit cycle until the time lag τ reaches a maximum value of $\tau_+ \approx 0.24562$.

Figures 1(a) and 1(b) represent the dynamics of time evolution of the host and tumor cells for the three cells fixed point E^* for $\tau_0 = 0.2342 > \overline{\tau} = 0.12$. For the lower threshold value of τ_0, model (2) demonstrates irregular long periodic oscillations. It is worthy to assume that a patient in stable situations would represent the parameters constant in time. Thus, it is possible to visualize different scenarios, only depending on patient situations, that is, on its set of parameters. We consider a patient with time delay $\tau_0 > \overline{\tau} = 0.12$, other parameters as reported in Table I. Assume that the patient has a single cancer site with few cancerous cells with initial values $x_0 = 0.1$, $y_0 = 0.55$, and $z_0 = 0.12$. The cycle-to-cycle variability of cancer populations is decreased by increasing the proliferation rate of host cells for $\tau_0 > \overline{\tau} = 0.12$, which means that the populations of host cells remain near its maximum value ($\approx$1) for

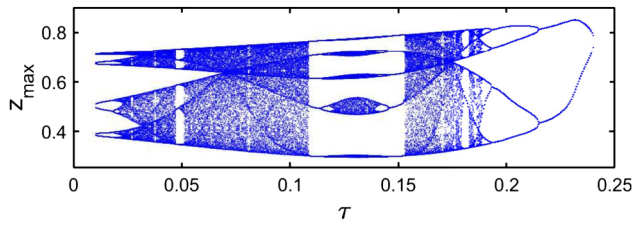

FIG. 3. Bifurcation diagram of the delayed tumor model (2) by changing the time lag τ. This figure shows that low and high values of τ the dynamics becomes regular and for $\tau > 0.24562$ the system becomes unbounded. Parameter values as specified in Table I.

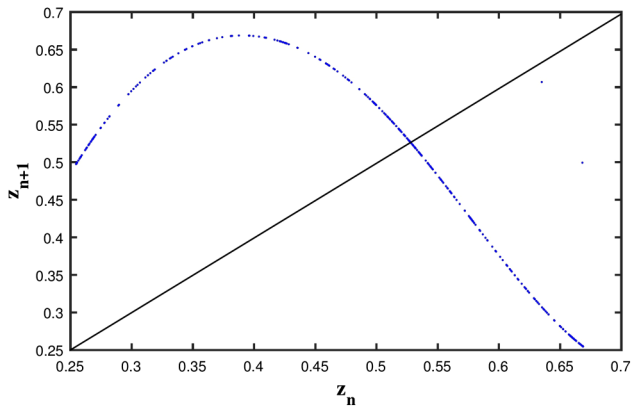

FIG. 4. The figure represents the smooth unimodal first-return map using Poincaré section of the chaotic attractor observed which shows period doubling route to chaos. The parameter values as specified in Table I with $\tau = 0.1$.

a small period of time and it is decreased quickly to zero [see Figs. 1(a) and 1(b)]. Consequently, the cancer cells remain near its lowest value ($\approx$0) and very quickly tumor cells proliferate and increased for a short period and then decreased. During this period of time, all the cells start to oscillate. If we look carefully, it can be observed that for the time delay $\tau_0 > \overline{\tau} = 0.12$, the oscillations are very small and asymmetrical (healthy cells remain at their highest value for a small period compared to cancer cells). Thus, for the fixed time delay $\tau_0 > \overline{\tau} = 0.12$, the host cells become strong enough to control the cancer cells. Unfortunately, the cancer cells grow very quickly for a small period and they destroy almost all healthy cells that assist to a detritus effect of cancer cells.

To investigate different patient situations, we decided to explore the parameter values, namely, the delay parameter τ and we noticed that it obeys to switch from a common to metastatic tumor, and the other parameters ρ, β_1, γ_1, and α. Bifurcation diagram against one of these parameters are plotted by using maxima and minima of the given variables to find its range of changeability. This has been established by a first-return map (see Fig. 4) to the Poincaré surface of section defined as

$$\mathcal{P} = \left[(z_n, \ddot{z}_n) \in \mathbb{R}^2 | \dot{z}_n = 0, \ddot{z}_n > 0\right].$$

The tumor model (2) demonstrates regular and asymmetrical periodic behaviors (chaotic dynamics) that has been plotted in Fig. 3 by changing the time lag τ. The bifurcation figure (see Fig. 3) begins with high periodic or chaotic behaviors.

For $0.0082 < \tau < 0.1931$, the tumor model (2) shows chaotic or high periodic nature that implies that the patients' situation is dependent on the time lag τ. For the lower critical level of $\overline{\tau} = 0.1391$, the cancer population shows malignancy or invasive behavior and the model behavior is entirely dependent on τ. For $0.0082 < \tau < 0.047$, the tumor model (2) exhibits chaotic or regular periodic behavior (see Fig. 3); for $0.047 < \tau < 0.051$, a narrow periodic window emerges in which the chaotic behavior reverts to periodic behavior and a small periodic window disappears via a cascade of period-doubling behaviors. If we further increased the value of time lag τ, for $0.051 < \tau < 0.1085$, the tumor model (2) indicates

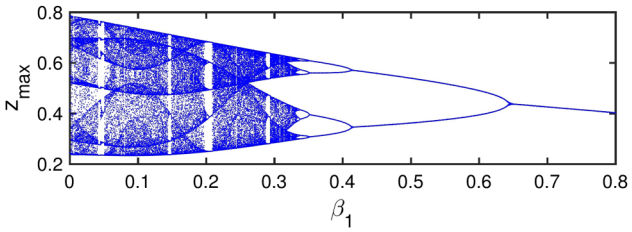

FIG. 5. Bifurcation diagram of the delayed system (2) with respect to the inhibition rate of the effector cells by tumor cells β_1 ($0.0 < \beta_1 < 0.8$) with $\tau = 0.12$. It is noted from this figure that the dynamics of cancer cells becomes more regular by higher inhibition rate β_1. Parameter values as specified in Table I.

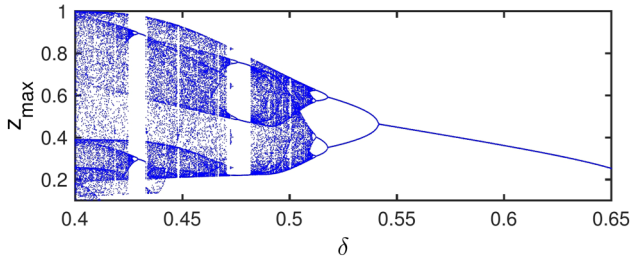

FIG. 6. Bifurcation diagram of the delayed system (2) by changing the natural death rate of effector cells δ ($0.4 < \delta < 0.65$). This figure signifies that the regular behavior of cancer cell is observed for higher values of natural death rate of effector cells. Other parameter values are given in Table I with $\tau = 0.12$.

chaotic behavior and again a large periodic window emerges for $0.1085 < \tau < 0.1531$ and a new periodic window disappears via a cascade of period-doubling behavior and this behavior persevere nearly at $\tau \approx 0.1931$. Moreover, for an increased magnitude of τ, the tumor model (2) becomes an attractor of period-8, an attractor of period-4, an attractor of period-2 and the tumor model eventually experiences a periodic limit cycle. For further increased value of τ, the tumor model (2) gains a fixed point which is stable in the equilibrium state, which implies that the cancer cells are dominated by the immune system. For lower threshold value of τ, the cancer cells become invasive and show malignant behavior, i.e., the patients' situations are controlled by the tumor cells but for a small increased value of τ, cancer cells stay under control and undergo the "dormant state." The first-return map to the Poincaré section $\mathcal{P}$ of this chaotic behavior is assembled by utilizing the variable z_n has been plotted in Fig. 4, which is a smooth unimodal map as awaited after the period-doubling cascade: certainly, a period-doubling bifurcation is necessarily connected with such a map.[33]

Similar conclusions can be addressed when the inhibition rate β_1 of effector cells is increased and we obtained the similar kind of bifurcation diagram (see Fig. 5) which we have already seen for the time lag τ. For the range of $\beta_1 \in (0, 0.3352)$, the tumor model (2) exhibits chaotic scenarios or high periodic behavior and the cancer cells are in the metastatic state. Many periodic windows appear in the range of $\beta_1 \in (0, 0.3352)$. In Fig. 5, the system is chaotic in the range $\beta_1 \in (0, 0.0416)$, and a narrow window appear in the range $\beta_1 \in (0.0416, 0.0512)$. In the range of the parameter $\beta_1 \in (0, 0.3352)$, model (2) has different periodic and chaotic attractors with many narrow windows. The highly periodic or chaotic region disappears at the threshold value $\beta_1 \approx 0.3352$ and the cancer proliferation is dominated by our immune system in the region of $\beta_1 \in (0.64, 0.8)$. Similar bifurcation figures (see Figs. 6 and 7) can be observed with reference to the parameter δ, γ_1, the natural decay rate of immune cells and the inhibition rate of host cells, respectively.

A model system is called chaotic if the trajectory created by its equations satisfy the property known as sensitive dependence on initial conditions.[28] Such property can also be noticed in the tumor growth dynamics,[11,12,28,29,33] and is presumed to be a sign of the existence of chaotic scenario in this system.[28] The most important indicator of chaotic dynamics that exhibits this property is the maximum Lyapunov Characteristic Exponent(LCE). If the maximum LCE of the trajectory created by a model is nonnegative, the model is chaotic in nature. A similarity among the stable, periodic, or chaotic phenomena can be achieved using bifurcation figures in Ref. 29. The bifurcation plot and maximum LCE spectrum for tumor system (2) with reference to the growth rate ρ of effector cells are demonstrated in Figs. 8(a) and 8(b), with parameter values as specified in Table I. There are different regions for the bifurcation plot [see Fig. 8(a)] and LCE [see Fig. 8(b)] for different ranges of the parameter ρ. This is summarized in Table II.

To understand the dynamics of cancer-immune competitive system, we compute two-dimensional bifurcation diagram as shown in Fig. 9. The 2-dimensional bifurcation plot is shown by the activation of immune cells due to cancer cells $\rho \in (3.5, 6.0)$ and discrete time delay $\tau \in (0, 0.25)$ (Fig. 9). For fixed value of time delay $\tau = 0.12$, increasing the value of ρ develops the dynamics, i.e., new stable periodic orbits are generated up to have a chaotic region (in the blue colored region). For fixed value of $\rho = 4.5$, for increasing value of τ, reverse bifurcation can be observed with unstable periodic solutions are pruned. From the oncological viewpoint, this would indicate that for an increasing value of τ with which the effector cells destroy cancer cells tends to decrease the resistance of the environment to cancer proliferation and thus would induce a poor prognostic. The 2-dimensional bifurcation figure helps us to indicate the regions where we minimize the oscillations for cancerous cells by managing the model parameters. Once the periodic behaviors, oscillations,

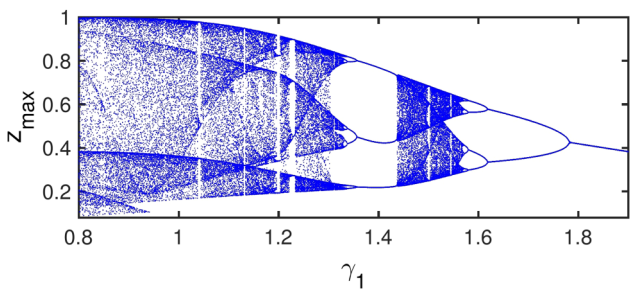

FIG. 7. Bifurcation diagram of tumor cell (z) in the delayed system (2) with respect to the host cell deactivation rate by tumor cells γ_1 ($0.8 < \gamma_1 < 2.0$) with $\tau = 0.12$. Inverse period doubling route to chaos is observed by increasing the value of γ_1. Parameter values as specified in Table I.

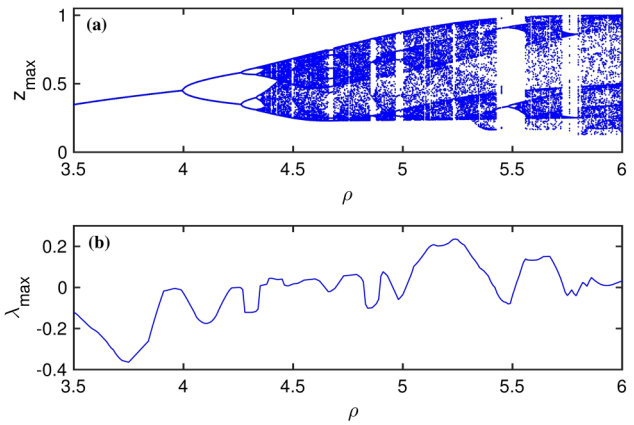

FIG. 8. The figures depict (a) the bifurcation diagram of the delayed model (2) versus the proliferation rate ρ of effector cells, and (b) variation of corresponding maximum Lyapunov Characteristics Exponent. Other parameter values are taken from Table I with $\tau = 0.12$.

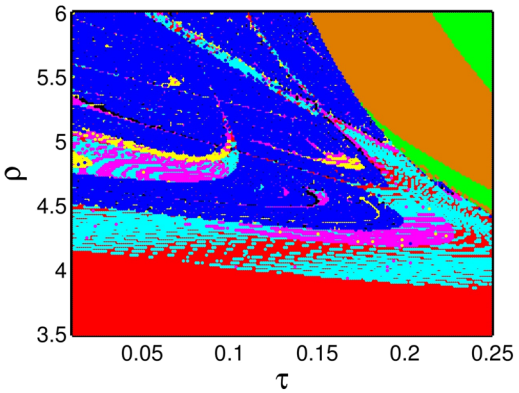

FIG. 9. The figure represents the two-dimensional bifurcation diagram for time delay $\tau \in (0, 0.25)$ versus the growth rate $\rho \in (3.5, 6.0)$ of effector cells for the model system (2). The color legends are used to represent different regions: red, limit cycle of period-1; cyan, limit cycle of period-2; magenta, limit cycle of period-3; yellow, limit cycle of period-4; black, limit cycle of period-5; blue, limit cycle of period ≥ 6 or chaotic attractor; brown, stable fixed point region; green, unbounded region. Parameter values as specified in Table I.

or periods are observed, the schedule for next remedy can be chalked out.

In order to study different patients' conditions, we varied two parameters, namely, the recruitment rate ρ of immune cells and the discrete time lag τ since we noticed that it allows to switch from normal to metastasis system and metastasis to dormant state. Now, we study the dynamics of the parameters α (proliferation rate of host cells), β_1 (rate of inhibition of immune cells), γ_1 (rate of inhibition of host cells), and δ (death rate of immune cells). The dynamics of the system (2), for the range $\alpha \in (0.4, 0.8)$ is well demonstrated using bifurcation diagram (see Fig. 10). In this range of $\alpha \in (0.4, 0.4898)$, the proliferation of cancer cell is well dominated by our immune system, and the cancer is in benign or non-malignant state. For $\alpha \in (0.4, 0.4616)$, the delayed model (2) has an exponential time dominating situation, reaching a stable equilibrium state. This is similar to spheroid cancer proliferation in an avascular stage that is exponential and at the end reaches the singular point. For $\alpha \in (0.4616, 0.4838)$, the interplay between cancer and immune system shows a periodic oscillation with limit cycle of period-1. For $\alpha \in (0.4838, 0.4885)$, the cancer and immune system interplay shows a periodic oscillation with limit cycle of period-2, and for $\alpha \in (0.4885, 0.4898)$, the tumor-immune system interaction leads to periodic behavior with limit cycle of period-4. For slightly increased value of α shows a high cancer burden in the system. It is known as the period-doubling cascade. Chaotic attractor noticed after the accumulation point (where the orbit 2^∞ happens) must therefore be characterized by a smooth unimodal map since a period-doubling cascade is the universal route to chaos in such a map.[45] At the proliferation rate $\alpha = 0.4898$ of host cells, a chaotic attractor or high periodic phenomena appears. Next, for the range of $\alpha \in (0.4898, 0.5108)$, the dynamics of the system is chaotic in nature, but in the chaotic region several narrow/large periodic scenarios can be noticed. The chaotic region converts to periodic behavior, similar to what occurs in the range of $\alpha \in (0.5108, 0.527)$. These narrow periodic window breaks down and disappears via the cascade of period-doubling bifurcations as the proliferation rate α of host cells is further increased. The period-doubling behavior is similar to the same mechanism which occurs in the range of $\alpha \in (0.527, 0.8)$, except that in the periodic windows.

TABLE II. Lyapunov characteristic exponent (LCE) for the tumor model (2) and system dynamics for different values of ρ.

Range of α	Sign of LCE	Attractor of the system
(3.500–3.995)	−	Fixed point
(3.995–4.265)	−	Period-1 limit cycle
(4.265–4.330)	−	Limit cycle of period-2
(4.330–4.350)	−	Limit cycle of period-4
(4.350–4.355)	−	Limit cycle of period-8
(4.355–4.490)	+	Chaotic (except periodic windows)
(4.490–4.505)	−	Limit cycle
(4.505–4.665)	+	Chaotic (except periodic windows)
(4.665–4.685)	−	Limit cycle
(4.685–4.855)	+	Chaotic (except periodic windows)
(4.855–4.882)	−	Limit cycle
(4.882–4.965)	+	Chaotic (except periodic windows)
(4.965–5.005)	−	Limit cycle
(5.005–5.435)	+	Chaotic (except periodic windows)
(5.435–5.565)	−	Limit cycle
(5.565–5.725)	+	Chaotic (except periodic windows)
(5.725–5.815)	−	Limit cycle
(5.815–6.000)	+	Chaotic (except periodic windows)

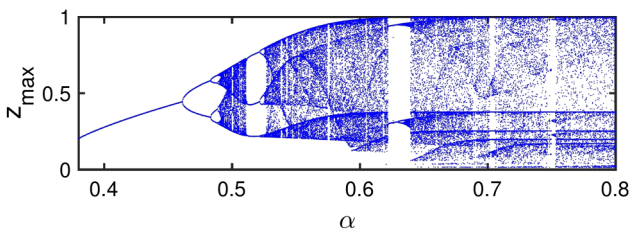

FIG. 10. Bifurcation diagram of the delayed system (2) by changing the proliferation rate α of the host cells with $\tau = 0.12$. Higher values of proliferation rate α influence the chaotic tumor dynamics. Other parameter values are given in Table I.

V. DISCUSSION

The interplay between cancer and immune system in the dynamics of cancer growth model is very intricated, which leads to various cancer growth pattern.[6,8,17,28] The model studied here is obviously a simplification of a complicated biological reality. In this manuscript, we studied a very simple and interesting mathematical model envisioned in de Pillis and Radunskaya.[36] The model investigates how cancerous cells evolve and survive the brief encounter with our immune system mediated by immune effector cells and host cells, with discrete time lag τ. Due to simple mathematical model some questions may arise that our tumor-immune model does not take into account the complicated immunological phenomena of tumor-immune interaction (cell types, genomic instability, expression of suppressive factors, etc.), but emphasizes on the generic interaction among different cells. Also, it is necessary to keep in mind that not all intricated mathematical models provide good dynamics and all information regarding cell interactions, and it simply complicates the model. An ideal model can give better insight into the dynamic relationship between cancer and immune responses and may play a vital role in understanding the dynamics of a cancer-immune interactions and designing preferable treatment policy. But, it is very difficult to develop realistic mathematical models to investigate such complicated immunological phenomenon. Certainly, mathematical model for the dynamic relationship between the cancer-immune responses are very idealized. Thus, it is important to design a simple mathematical model which allows ample complexities, that can capture most of the important immunological phenomenon.

In our delayed system (2), we provide detailed analysis of the positivity for the systems, boundedness of the solutions, and the local stability for the biologically realistic singular points. By using time lag as a bifurcation parameter, we performed Hopf bifurcation analysis. We calculate the length of time delay τ to maintain the stability of limit cycle of period-1 arising from Hopf bifurcation. The newness of the tumor model is to incorporate a time lag to well understand the complicated biological phenomenon. Using normal form theorem and the theory of center manifold, precise aspect for the direction of Hopf bifurcation and the stability of bifurcating periodic solutions are acquired. We explored some numerical integrations of the system to validate our theoretical observations. Roughly speaking, the nonnegative fixed point E^* is asymptotically stable when the discrete time lag τ is less than their corresponding threshold value. The nonnegative singular point E^* becomes unstable and the tumor model (2) undergoes Hopf bifurcation if the time lag τ crosses through its threshold value. Our analytical findings and numerical integrations exhibit that the nonlinear interplay of the cancer-immune competitive system with single discrete time lag is very complicated and difficult to explore even for the simple case when there is only one nonnegative singular point. The significance of Hopf bifurcation subject to the tumor-immune interaction is that, at the bifurcation state a limit cycle appears around the singular point, therefore, resulting in a stable periodic oscillation. Furthermore, the stability of bifurcating limit cycle of period-1 persists up to $\tau_+ = 0.24562$. The appearance of periodic behaviors has a medical confirmation in cancer dynamics, as it is verified that the cancer levels may swing surrounding the singular point even in exclusion of any therapy. Such type of scenario is called as "Jeff's phenomena."[42]

Our delayed model (2) exhibits more complex dynamical behavior which has been observed in the numerical section by varying the discrete time lag τ as well as the model parameters, namely, ρ, β_1, α, δ, γ_1, and γ_2. The mathematical model under consideration has a very interesting dynamics which demonstrate stable symmetrical and asymmetrical long periodic behaviors (high periodic or chaotic scenarios) for the different set of system parameters. The most interesting thing of this article is to explore the bifurcation figure for single parameter and the two parameter bifurcations and stability region. Through 2-dimensional bifurcation diagrams, we recognize the region of singular points, limit cycles, periodic oscillations, and highly periodic or chaotic attractors.

The models have the ability to exhibit the existence of chaotic behaviors in the cancer-immune competitive system (delayed as well as non-delayed system), some examples[10,12,29,37] are in continuous models. Our model system (2) exhibits chaotic dynamics which has been verified by the most important indicator for chaotic dynamics is the maximum Lyapunov Characteristic Exponent(LCE). If the maximum LCE of the trajectory created by a tumor model is nonnegative, the system shows chaotic behavior. The bifurcation plot and the LCE spectrum for the tumor model (2) with reference to the proliferation rate ρ of immune cells are demonstrated in Figs. 8(a) and 8(b), with parameter values are reported in Table I. The appearance of regular and asymmetric periodic oscillations, chaotic behavior in the cancer-immune competitive system demonstrates the scenario of long-term cancer relapse which has been investigated in some related cancer-immune interaction models.[10,12,28,37]

Using the numerical simulations, the unforeseeable proliferation of cancer populations in vivo and the experimental investigations can be interpreted. Our mathematical model exhibits for both the large and small cancer burden which have oscillatory dynamics. By changing the system parameters in a broad range, the interplay among tumor-immune interplay demonstrates more complicated dynamics like regular and irregular periodic behaviors and random like chaotic or high periodic scenarios. The regular periodic behaviors indicate the equilibrium process (expansion of transformed cells) of tumor immunoediting in the dual host-protective and cancer-promoting actions of immunity and support the clinical investigations by Koebel *et al.*[24] The occurrence of asymmetric long periodic behavior indicates that with temporal delay in the immune response tumor may develop to a more hostile situation. It would be fascinating to find oncological or immunological data on cancer-immune competitive system and see if our modeling outcomes and simulations verify to the data. Like other analogous kind of mathematical models, our tumor model also does not take into account to investigate the particular type of cancer. Also, our tumor model is very elementary contrast to real tumor evolution. Therefore, the tumor model must be modified by utilizing the outcomes of experimental observations and adding some particular cells

like NK cells, macrophages, stem cells, myeloid cells, and cytokines like IL-10, IL-21, and IFN-γ, etc.

ACKNOWLEDGMENTS

Matjaž Perc was supported by the Slovenian Research Agency (Grant Nos. J1-7009, J4-9302, J1-9112, and P5-0027).

[1]L. M. F. Merlo, J. W. Pepper, B. J. Reid, and C. C. Maley, Nat. Rev. Cancer **6**, 924–935 (2006).
[2]R. A. Gatenby and P. K. Maini, Nature **421**, 321 (2003).
[3]J. Adam and N. Bellomo, *A Survey of Models for Tumor Immune Dynamics* (Birkhauser, Boston, 1997).
[4]S. Khajanchi and D. Ghosh, Appl. Math. Comput. **271**, 375–388 (2015).
[5]R. P. Araujo and D. L. S. McElwaina, Bull. Math. Biol. **66**, 1039–1091 (2004).
[6]V. A. Kuznetsov, I. A. Makalkin, M. A. Taylor, and A. S. Perelson, Bull. Math. Biol. **56**(2), 295–321 (1994).
[7]R. H. Thomlinson and L. J. Gray, Br. J. Cancer **9**, 539–549 (1955).
[8]S. Banerjee, S. Khajanchi, and S. Chaudhury, PLoS One **10**(5), e0123611 (2015).
[9]C. Letellier, S. K. Sasmal, C. Draghi, F. Denis, and D. Ghosh, Chaos Solitons Fractals **99**, 297–311 (2017).
[10]P. Bi, S. Ruan, and X. Zhang, Chaos **24**, 023101 (2014).
[11]S. Khajanchi and S. Banerjee, Appl. Math. Comput. **248**, 652–671 (2014).
[12]C. Letellier, F. Denis, and L. A. Aguirre, J. Theor. Biol. **322**, 7–16 (2013).
[13]S. Khajanchi and J. J. Nieto, Appl. Math. Comput. **340**, 180–205 (2019).
[14]E. F. Wheelock, K. J. Weinhold, and J. Levich, Adv. Cancer Res. **34**, 107–140 (1981).
[15]A. Robertson-Tessi, A. El-Kareh, and A. Goriely, J. Theor. Biol. **249**, 56–73 (2012).
[16]S. Khajanchi and S. Banerjee, Math. Biosci. **289**, 69–77 (2017).
[17]E. Ahmed, Int. J. Theor. Phys. **32**(2), 353–355 (1992).
[18]A. El-Gohary, Chaos Soliton Fractals **37**(5), 1305–1316 (2008).
[19]M. Villasana and A. Radunskaya, J. Math. Biol. **47**, 270–294 (2003).
[20]N. E. Lorenz, J. Atmos. Sci. **20**(2), 130–148 (1963).
[21]G. P. Dunn, A. T. Bruce, H. Ikeda, L. J. Old, and R. D. Schreiber, Nat. Immunol. **3**, 991–998 (2002).
[22]G. P. Dunn, L. J. Old, and R. D. Schreiber, Annu. Rev. Immunol. **22**, 329–360 (2004).
[23]S. Khajanchi, Biophys. Rev. Lett. **12**(4), 187–208 (2017).
[24]C. M. Koebel, W. Vermi, J. B. Swann, N. Zerafa, S. Rodig, L. J. Old, M. J. Smyth, and R. D. Schreiber, Nature **450**, 903–907 (2007).
[25]M. D. Vesely, M. H. Kershaw, R. D. Schreiber, and M. J. Smyth, Annu. Rev. Immunol. **29**, 235–271 (2011).
[26]D. Ghosh, A. Roy Chowdhury, and P. Saha, Chaos Solitons Fractals **35**, 472–485 (2008).
[27]D. Ghosh, Chaos **19**, 013102 (2009).
[28]M. Moghtadaei, M. R. H. Golpayegani, and R. Malekzadeh, J. Theor. Biol. **334**, 130–140 (2013).
[29]S. Khajanchi, Chaos Solitons Fractals **77**, 264–276 (2015).
[30]H. M. Byrne, Math. Biosci. **144**, 83–117 (1997).
[31]A. d'Onofrio, F. Gatti, P. Cerrai, and L. Freshi, Math. Comput. Model. **51**, 572–591 (2010).
[32]U. Forys and M. J. Piotrowska, Appl. Math. Comput. **220**, 277–295 (2013).
[33]D. Ghosh, S. Khajanchi, S. Mangiarotti, F. Denis, S. K. Dana, and C. Letellier, BioSystems **158**, 17–30 (2017).
[34]S. Khajanchi and S. Banerjee, Math. Biosci. **302**, 116–130 (2018).
[35]M. J. Piotrowska, M. Bodnar, J. Poleszczuk, and U. Forys, Nonlinear Anal. Real World Appl. **14**, 1601–1620 (2013).
[36]L. G. de Pillis and A. Radunskaya, Math. Comput. Model. **37**, 1221–1244 (2003).
[37]M. Itik and S. P. Banks, Int. J. Bifurcat. Chaos **20**(1), 71–79 (2010).
[38]S. Khajanchi, Chaos Solitons Fractals **114**, 108–118 (2018).
[39]S. L. Topalian *et al.*, N. Eng. J. Med. **24**(26), 2443–2454 (2012).
[40]R. Eftimie, J. L. Bramson, and D. J. D. Earn, Bull. Math. Biol. **73**, 2–32 (2011).
[41]S. R. McDougall, A. R. A. Anderson, and M. A. J. Chaplain, J. Theor. Biol. **241**(3), 564–589 (2006).
[42]R. Thomlinson, Clin. Radiol. **33**, 481–493 (1982).
[43]H. I. Freedman and V. S. H. Rao, Bull. Math. Biol. **45**(6), 991–1004 (1983).
[44]K. Cooke and P. van den Driessche, J. Math. Biol. **35**, 240–260 (1996).
[45]M. J. Feigenbaum, J. Stat. Phys. **19**, 25–52 (1978).